ChemComm

COMMUNICATION

View Article Online
View Journal | View Issue

Cite this: *Chem. Commun.*, 2019, **55**, 5147

Received 8th March 2019,
Accepted 8th April 2019

DOI: 10.1039/c9cc01898k

rsc.li/chemcomm

Role of hydrophobic residues for the gaseous formation of helical motifs†

Lin Liu,[a] Xin Dong,[a] Yichang Liu,[a] Nicklas Österlund,[b] Astrid Gräslund,[b] Paolo Carloni*[c] and Jinyu Li*[a]

The secondary structure content of proteins and their complexes may change significantly on passing from aqueous solution to the gas phase (as in mass spectrometry experiments). In this work, we investigate the impact of hydrophobic residues on the formation of the secondary structure of a real protein complex in the gas phase. We focus on a well-studied protein complex, the amyloid-β (1-40) dimer (2Aβ). Molecular dynamics simulations reproduce the results of ion mobility-mass spectrometry experiments. In addition, a helix (not present in the solution) is identified involving ^{19}FFAED^{23}, consistent with infrared spectroscopy data on an Aβ segment. Our simulations further point to the role of hydrophobic residues in the formation of helical motifs – hydrophobic sidechains "shield" helices from being approached by residues that carry hydrogen bond sites. In particular, two hydrophobic phenylalanine residues, F19 and F20, play an important role for the helix, which is induced in the gas phase in spite of the presence of two carboxyl-containing residues.

Native mass spectrometry (MS) allows the native structures of biomolecules to be probed in a vacuum.[1] A great deal has been clarified about how molecular structures change on passing from water to the gas phase.[2,3] With the help of soft ionization techniques, ion mobility-MS (IM-MS) can reveal the global geometry of biomolecules and their complexes, *via* the measured charge state distribution and the collisional cross section (CCS).[4–6] However, these observables determined by IM-MS are not sensitive to the protein secondary structure. To gain such information it has been proposed to couple IM-MS with infrared (IR) spectroscopy.[7,8] The latter can provide a characteristic vibrational fingerprint that is sensitive to the protein secondary structure.[9,10] A number of experimental works have witnessed that helical motifs are likely to exist in the gas phase under mild conditions.[11–13] Unfortunately, the association of IM-MS and IR spectroscopy alone cannot provide information about where and how such helices are embedded in proteins, as well as the molecular mechanism of the formation and stabilization of helices in the gas phase. The shortcomings can be circumvented with the aid of computational methods.

Extensive molecular simulation is a powerful way to render such missing information. It is capable of disclosing the structural and dynamic behaviors of proteins in the gas phase, as already demonstrated by several groups including ours.[14–18] In this context, we apply a multiple-step computational protocol integrating long-timescale (sub-millisecond) molecular dynamics (MD) and hybrid Monte Carlo (MC)/MD simulations on a protein complex, the amyloid-β (1-40) dimer (2Aβ hereafter). Aβ is an intrinsically disordered protein, and its dimer is the smallest neurotoxic oligomeric species related to Alzheimer's disease *in vivo*.[19,20] The secondary structural pattern of proteins is strongly modulated by the embedded environment. Given that the helicity of Aβ may increase under non-hydrophilic conditions, we are curious whether such conversion occurs in the gas phase.[21]

We first investigate the conformational ensembles of 2Aβ in aqueous solution. The starting structure of 2Aβ is generated using the protocol reported before for the investigation of Aβ dimerization (see details in the ESI†).[22] Three 2 μs-long independent MD simulations with different initial microscopic conditions are carried out on 2Aβ. Three conformational ensembles ($E1_s$, $E2_s$, and $E3_s$ hereafter) are consequently obtained by cluster analysis (Fig. S1–S3, ESI†). Secondary structure analysis shows that 2Aβ contains a significant amount of flexible turn and coil components (80.6 ± 4.9%) in aqueous solution (Table S1, ESI†). In addition, the β component (12.2 ± 4.9%) is more abundant over the helix (7.2 ± 0.4%), which is in good agreement with previous circular dichroism spectrum results (3% for the helix and 13% for the β content)

[a] *College of Chemistry, Fuzhou University, 350002 Fuzhou, China. E-mail: j.li@fzu.edu.cn*
[b] *Department of Biochemistry and Biophysics, Arrhenius Laboratories, Stockholm University, 106 91 Stockholm, Sweden*
[c] *Computational Biomedicine, Institute for Advanced Simulation IAS-5 and Institute of Neuroscience and Medicine INM-9, Forschungszentrum Jülich, 52425 Jülich, Germany. E-mail: p.carloni@fz-juelich.de*

† Electronic supplementary information (ESI) available. See DOI: 10.1039/c9cc01898k

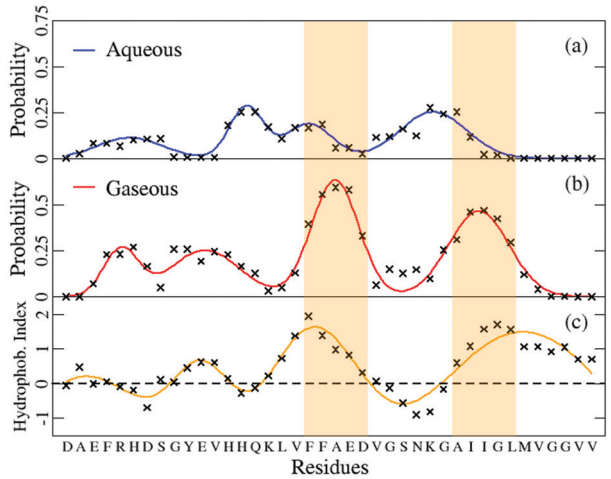

Fig. 1 Helical probability plot using residues of Aβ in the aqueous phase (a) and in the gas phase (b), together with the plot of the hydrophobicity index by residue (c). Helical regions predicted in MD simulations are highlighted in colored strips.

and recent MD studies (10% for the helix and 17% for the β content).[23–25] We notice that the locations of the specific secondary structure are diverse among three conformational ensembles. For example, a β hairpin motif that appears from F20 to G25 is observed in the $E1_s$ ensemble while they are random coils in others (Fig. S3, ESI†). It is not possible to find any helical region across the dimer when considering all ensembles, *i.e.* the probabilities of residues to be helical are all below 30% (Fig. 1a). This fulfills the intrinsically disordered nature of Aβ and meanwhile suggests that our simulations are not biased toward a specific pattern of folding.

Let us now describe 2Aβ conformational ensembles in the gas phase. We focus on the main charge state, 5+, as measured in IM-MS experiments.[26] The lowest-energy protonation states of 2Aβ with a total charge of 5+ are first predicted for each representative aqueous conformer (from $E1_s$, $E2_s$, and $E3_s$, respectively) using a well-established hybrid MC/MD protocol, which has been proved effective on structured proteins and intrinsically disordered peptides (Fig. S4, see the ESI† for details).[14] Intriguingly, we find two favorable protonation states for $E1_s$, *i.e.* the gas-phase basicity-corrected energy of the two states is within the reported energy cutoff for the MC/MD protocol (125 kJ mol^{-1}).[14] It is in agreement with our previous B3LYP-based quantum mechanics/molecular mechanics simulations on the N-terminal Aβ (1-16) segment, where different protonation states may co-exist in the gas phase and transform *via* proton transfer reactions.[15] For $E2_s$ and $E3_s$, only one lowest-energy protonation state is identified. Subsequently, four 200 μs-long gaseous MD simulations of 2Aβ are carried out with the representative aqueous conformers and corresponding protonation states identified above. These simulations generate four representative conformational ensembles of 2Aβ ($E1a_g$, $E1b_g$, $E2_g$, and $E3_g$ hereafter). Our simulations are consistent with the fact that the conformational flexibility of Aβ in the gas phase is a reflection of its intrinsically disordered nature in the aqueous solution.[27] Although these ensembles are distinctive in structure (Fig. S1, S2, and S5, ESI†), their CCS values (1241 ± 13, 1256 ± 14, 1270 ± 12, and 1239 ± 11 $Å^2$), calculated using the trajectory method, are very similar.[28] Given that the CCS shows an approximate 3% experimental error, the calculated values of 2Aβ are in quantitative agreement with the IM-MS one (1226 $Å^2$) recently reported by Heo *et al.*[29] In spite of the success in capturing global geometry through the observable CCS, our simulations indicate that the CCS may not be sensitive enough to reflect the structural differences among co-existing conformational ensembles of 2Aβ in the gas phase.

The principal secondary structural components of 2Aβ in the gas phase remain as turn and random coils, indicating that the intrinsically disordered nature of the protein complex is conserved in the vacuum (Table S2, ESI†). The secondary structure content, however, changes drastically: the β component (4.6 ± 4.1%) becomes less popular than that in the aqueous phase. Instead, the helix component (20.6 ± 4.9%) increases. The helix probability plot (Fig. 1b) shows that, in contrast to the aqueous solution case, two helices are likely to form. The first is a partially hydrophobic 3_{10} helix (sequence ^{19}FFAED^{23}), featuring two consecutive $i \rightarrow i - 3$ hydrogen bonds, between E22 and F19 and between D23 and F20 (Fig. 2). Notably, this helical region has been observed in previous IR-incorporated MS experiments on the Aβ (12-28) peptide segment.[30–32] The second is completely hydrophobic (sequence ^{30}AIIGL^{34}). It forms two backbone hydrogen bonds, between G33 and A30 and between L34 and I31 (Fig. S6, ESI†).

Overall, both helical regions contain at least 60% hydrophobic residues. This contrasts with the non-helical regions, which contain only 33% hydrophobic residues. The hydrophobic index by residue displays a clear correlation to the gaseous helical probability (Fig. 1b and c). There are two hydrophobic bands in Aβ, where the indexes are higher than one. Interestingly, the helical regions and the hydrophobic bands broadly overlap each other. This suggests that hydrophobic side chains may be important for the formation of helices in the gas phase.

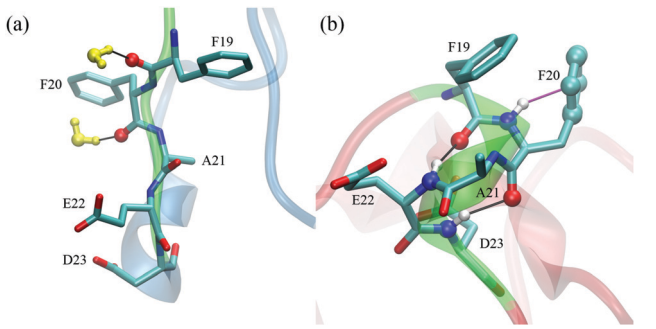

Fig. 2 Selected local conformer of 2Aβ in the aqueous phase (a) and in the gas phase (b). The 19FFAED23 region is highlighted in transparent green. Carbon atoms are colored in cyan, hydrogen atoms are in white, oxygen atoms are in red, and nitrogen atoms are in blue. Solvent water molecules are colored in yellow. (π) Hydrogen bonds are depicted as black (purple) continuous lines. Only hydrogen atoms forming these interactions are shown.

Indeed, we show here that hydrophobic sidechains "shield" helices from being approached by other residues that carry hydrogen bond sites.

In the aqueous solution, water molecules reduce the likelihood of intramolecular hydrogen bonds between backbone units. Notably, backbone carbonyl groups from hydrophobic residues form 0.84 ± 0.02 hydrogen bonds on average with water. In contrast, the carbonyl groups form only 0.70 ± 0.04 hydrogen bonds for the rest of the residues. For F19 and F20, the number is even higher (0.91 ± 0.04). One plausible reason is that carbonyl groups point towards the protein–water interface (Fig. 2). Due to the hydrophobic effect, it is thermodynamically unfavorable for hydrophobic sidechains to contact water molecules at the interface. The competition of hydrogen bond formation with water molecules can interfere with the stability of backbone hydrogen bonds, which explains why we did not observe definite helical motifs in the aqueous phase.

On passing from the aqueous solution to the gas phase, we notice that intramolecular hydrogen bonds dramatically increase (from 32.9 ± 1.5 to 51.0 ± 2.1). Such an observation agrees with a number of previous studies, in which intramolecular hydrogen bonds of biomolecules increase after vaporization.[14,33,34] Kondalaji *et al.* rationalized that, within helical motifs, the extent and the duration of hydrogen bonds enhance in the solvent-free vacuum environment.[33] Li *et al.* and Konermann independently confirmed the appearance of new hydrogen bonds and salt bridges in protein complexes under MS conditions.[14,34]

The residue-residue contacts increase from 1.2 to 1.5 on passing from water to the gas phase (see the definition of contact in the ESI†). This is consistent with the previous experiments and simulations, which have demonstrated that proteins can collapse in the structure under the condition of the gas phase.[35,36] However, the contacts are sparse concerning both helical regions (Fig. 3 and Fig. S7, ESI†). This clearly shows that a number of intermolecular contacts disappear in such regions with phase transition, as highlighted in boxes (Fig. 3). We attribute this to the sidechain hydrophobicity. Hydrophobic sidechains lack hydrogen bond sites, explicit charges, or local dipole moments. In the aqueous solution, the hydrophobic sidechains form contacts *via* van der Waals and hydrophobic interactions. Nonetheless, in the gas phase, the situation is different. The formation of new hydrogen bonds and salt bridges induces more contacts for hydrophilic sidechains (Fig. S7, ESI†). This is not the case for hydrophobic sidechains. Besides, the existing contacts of hydrophobic sidechains become unstable, because the van der Waals interaction is relatively weak. The contact numbers drop from 1.0 to 0.7 for each hydrophobic residue while they rise from 1.3 to 2.1 for the non-hydrophobic residue, suggesting that strong interactions may easily override the weak van der Waals interaction. Moreover, the existing hydrophobic residues are reluctant to attract residues that bear hydrogen bond sites, thereby preventing hydrogen bonds at helical regions from being disrupted.

Finally, the backbone N–H bonds of F19 and F20 from the first helix, at times, point toward the corresponding phenyl rings and form π hydrogen bonds (Fig. 2b). The π hydrogen

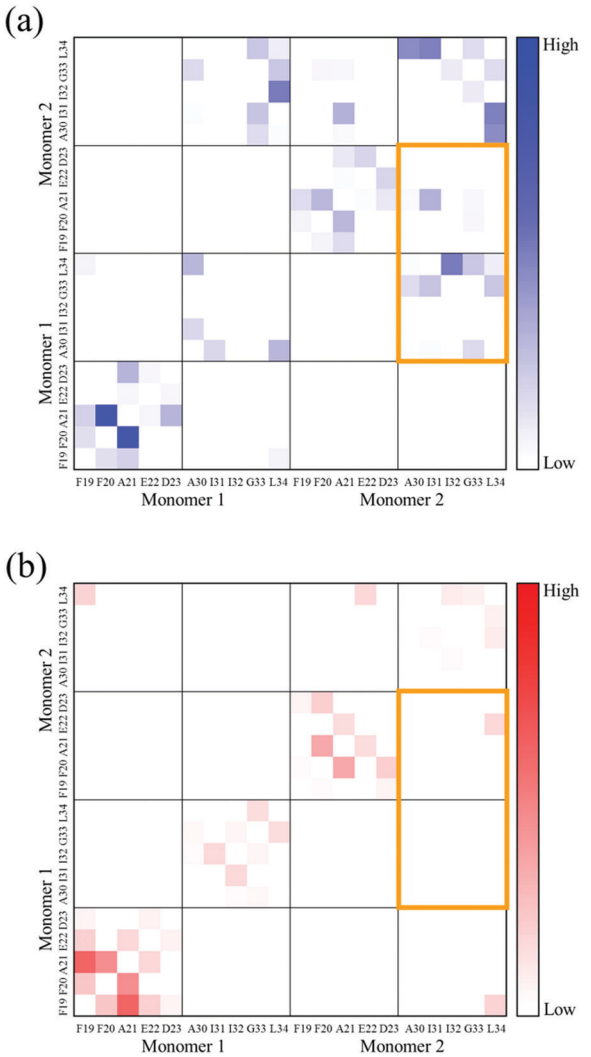

Fig. 3 Sidechain contact maps of regions with high helical probability as obtained from our simulations in the aqueous phase (a) and in the gas phase (b). Orange boxes highlight the conformation evolution of phase transition.

bonds were also present in previous experimental and computational studies on a model peptide of polyalanine (sequence Ac-FAAAAAK).[37,38] It has been validated that the N-terminal capping of the phenylalanine residue can stabilize the gaseous helical motif. In order to elucidate the contribution of the hydrophobic effect and π hydrogen bonds to the formation of gas-phase helices, we conduct MD simulations on two mutants, in which two phenylalanine residues are replaced with double alanine (FΔA) and glycine (FΔG) residues, respectively. For the FΔA mutant (sequence ^{19}AAAED^{23}), the helix propensities at this region slightly decrease, as the alanine sidechain is hydrophobic. For the FΔG mutant (sequence ^{19}GGAED^{23}), however, such values significantly decline, emphasizing the pivotal role of hydrophobicity (Table S3, ESI†). Indeed, we observe that, after the removal of phenylalanine sidechains, the protonated carboxyl group of D23 is hydrogen-bonded to the carbonyl group of G19, disturbing the helical hydrogen bond network (Fig. S8, ESI†).

From native MS experiments, it is not clear whether the secondary structure units in the gas phase are embedded in the same manner as in the aqueous solution.[12] Indeed, our simulations show that overall geometry and the secondary structure component may evolve on transferring from aqueous solution to the gas phase. In conclusion, we have presented the gaseous structure of 2Aβ as predicted by extensive MD simulations. The simulation results are validated by a comparison with available IM-MS and IR experimental data, respectively. They show that hydrophobic residues impact significantly on the formation and stabilization of helical motifs in the gas phase. Hydrophobic sidechains keep helices from being approached by other residues that carry hydrogen bond sites. Interestingly, the two hydrophobic phenylalanine residues assist the formation of a helix in spite of the presence of two carboxyl-group-containing residues. Hence, this work not only complements previous experimental observations but also provides insight into intriguing aspects of gas phase structural biology.

We gratefully acknowledge the financial support from the National Natural Science Foundation of China (grant no. 21603033). L. L. appreciates the help of Dr Hugh Kim from Korea University.

Conflicts of interest

There are no conflicts to declare.

Notes and references

1 S. A. Chandler and J. L. Benesch, *Curr. Opin. Chem. Biol.*, 2018, **42**, 130.
2 K. A. Servage, J. A. Silveira, K. L. Fort and D. H. Russell, *Acc. Chem. Res.*, 2016, **49**, 1421.
3 T. Wyttenbach, N. A. Pierson, D. E. Clemmer and M. T. Bowers, *Annu. Rev. Phys. Chem.*, 2014, **65**, 175.
4 J. Li, C. Santambrogio, S. Brocca, G. Rossetti, P. Carloni and R. Grandori, *Mass Spectrom. Rev.*, 2016, **35**, 111.
5 D. Stuchfield and P. Barran, *Curr. Opin. Chem. Biol.*, 2018, **42**, 177.
6 V. Gabelica and E. Marklund, *Curr. Opin. Chem. Biol.*, 2018, **42**, 51.
7 W. Hoffmann, G. von Helden and K. Pagel, *Curr. Opin. Struct. Biol.*, 2017, **46**, 7.
8 L. Voronina, V. Scutelnic, C. Masellis and T. R. Rizzo, *J. Am. Chem. Soc.*, 2018, **140**, 2401.
9 A. Ghosh, J. S. Ostrander and M. T. Zanni, *Chem. Rev.*, 2017, **117**, 10726.
10 M. Z. Kamrath and T. R. Rizzo, *Acc. Chem. Res.*, 2018, **51**, 1487.
11 S. J. C. Lee, J. W. Lee, T. S. Choi, K. S. Jin, S. Lee, C. Ban and H. I. Kim, *Anal. Chem.*, 2014, **86**, 1909.
12 J. Seo, W. Hoffmann, S. Warnke, M. T. Bowers, K. Pagel and G. von Helden, *Angew. Chem., Int. Ed.*, 2016, **55**, 14173.
13 S. Warnke, W. Hoffmann, J. Seo, E. De Genst, G. von Helden and K. Pagel, *J. Am. Soc. Mass Spectrom*, 2017, **28**, 638.
14 J. Y. Li, G. Rossetti, J. Dreyer, S. Raugei, E. Ippoliti, B. Luscher and P. Carloni, *PLoS Comput. Biol.*, 2014, **10**, e1003838.
15 J. Y. Li, W. P. Lyu, G. Rossetti, A. Konijnenberg, A. Natalello, E. Ippoliti, M. Orozco, F. Sobott, R. Grandori and P. Carloni, *J. Phys. Chem. Lett.*, 2017, **8**, 1105.
16 G. Ben-Nissan and M. Sharon, *Curr. Opin. Chem. Biol.*, 2018, **42**, 25.
17 W. F. van Gunsteren, J. R. Allison, X. Daura, J. Dolenc, N. Hansen, A. E. Mark, C. Oostenbrink, V. H. Rusu and L. J. Smith, *Angew. Chem., Int. Ed.*, 2016, **55**, 15990.
18 L. Konermann, H. Metwally, R. G. McAllister and V. Popa, *Methods*, 2018, **144**, 104.
19 G. M. Shankar, S. M. Li, T. H. Mehta, A. Garcia-Munoz, N. E. Shepardson, I. Smith, F. M. Brett, M. A. Farrell, M. J. Rowan, C. A. Lemere, C. M. Regan, D. M. Walsh, B. L. Sabatini and D. J. Selkoe, *Nat. Med.*, 2008, **14**, 837.
20 S. J. C. Lee, E. Nam, H. J. Lee, M. G. Savelieff and M. H. Lim, *Chem. Soc. Rev.*, 2017, **46**, 310.
21 A. Wahlstrom, L. Hugonin, A. Peralvarez-Marin, J. Jarvet and A. Graslund, *FEBS J.*, 2008, **275**, 5117.
22 S. H. Chong and S. Ham, *Proc. Natl. Acad. Sci. U. S. A.*, 2012, **109**, 7636.
23 G. Bitan, M. D. Kirkitadze, A. Lomakin, S. S. Vollers, G. B. Benedek and D. B. Teplow, *Proc. Natl. Acad. Sci. U. S. A.*, 2003, **100**, 330.
24 B. Tarus, T. T. Tran, J. Nasica-Labouze, F. Stepone, P. H. Nguyen and P. Derreumaux, *J. Phys. Chem. B*, 2015, **119**, 10478.
25 P. H. Nguyen, F. Sterpone, R. Pouplana, P. Derreumaux and J. M. Campanera, *J. Phys. Chem. B*, 2016, **120**, 12111.
26 M. Kloniecki, A. Jablonowska, J. Poznanski, J. Langridge, C. Hughes, I. Campuzano, K. Giles and M. Dadlez, *J. Mol. Biol.*, 2011, **407**, 110.
27 A. S. Phillips, A. F. Gomes, J. M. D. Kalapothakis, J. E. Gillam, J. Gasparavicius, F. C. Gozzo, T. Kunath, C. MacPhee and P. E. Barran, *Analyst*, 2015, **140**, 3070.
28 M. F. Mesleh, J. M. Hunter, A. A. Shvartsburg, G. C. Schatz and M. F. Jarrold, *J. Phys. Chem.*, 1996, **100**, 16082.
29 C. E. Heo, T. S. Choi and H. I. Kim, *Int. J. Mass Spectrom.*, 2018, **428**, 15.
30 T. N. Le, J. C. Poully, F. Lecomte, N. Nieuwjaer, B. Manil, C. Desfrancois, F. Chirot, J. Lemoine, P. Dugourd, G. van der Rest and G. Gregoire, *J. Am. Soc. Mass Spectrom*, 2013, **24**, 1937.
31 S. Daly, A. Kulesza, F. Poussigue, A. L. Simon, C. M. Choi, G. Knight, F. Chirot, L. MacAleese, R. Antoine and P. Dugourd, *Chem. Sci.*, 2015, **6**, 5040.
32 A. Kulesza, S. Daly, C. M. Choi, A. L. Simon, F. Chirot, L. MacAleese, R. Antoine and P. Dugourd, *Phys. Chem. Chem. Phys.*, 2016, **18**, 9061.
33 S. G. Kondalaji, M. Khakinejad and S. J. Valentine, *J. Am. Soc. Mass Spectrom*, 2018, **29**, 1665.
34 L. Konermann, *J. Phys. Chem. B*, 2017, **121**, 8102.
35 F. Lanucara, S. W. Holman, C. J. Gray and C. E. Eyers, *Nat. Chem.*, 2014, **6**, 281.
36 D. Stuchfield and P. Barran, *Curr. Opin. Chem. Biol.*, 2018, **42**, 177.
37 J. A. Stearns, O. V. Boyarkin and T. R. Rizzo, *J. Am. Chem. Soc.*, 2007, **129**, 13820.
38 J. A. Stearns, C. Seaiby, O. V. Boyarkin and T. R. Rizzo, *Phys. Chem. Chem. Phys.*, 2009, **11**, 125.

